PHYSICAL REVIEW C **85**, 051602(R) (2012)

Effect of isospin-dependent cluster recognition on the observables in heavy ion collisions

Yingxun Zhang (张英逊),[1] Zhuxia Li (李祝霞),[1] Chengshuang Zhou (周承双),[1,2] and M. B. Tsang (曾敏兒)[3]
[1]*China Institute of Atomic Energy, Post Office Box 275 (10), Beijing 102413, China*
[2]*College of Physics and Technology,Guangxi Normal University, Guilin 541004,China*
[3]*National Superconducting Cyclotron Laboratory and Joint Institute of Nuclear Astrophysics, Michigan State University, East Lansing, Michigan 48824, USA*
(Received 27 March 2012; published 22 May 2012)

We introduce isospin dependence in the cluster recognition algorithms used in the quantum molecular dynamics model to describe fragment formation in heavy ion collisions. This change reduces the yields of emitted nucleons and enhances the yields of fragments, especially heavier fragments. The enhancement of neutron-rich lighter fragments mainly occurs at midrapidity. Consequently, isospin-dependent observables, such as isotope distributions, yield ratios of n/p, $t/^3$He, and isoscaling parameters are affected. We also investigate how equilibration in heavy ion collisions is affected by this change.

DOI: 10.1103/PhysRevC.85.051602 PACS number(s): 25.70.Mn, 21.65.Ef, 24.10.Lx, 25.70.Pq

The productions of nucleons, light particles, and intermediate mass fragments (IMFs) in heavy ion collisions (HICs) provide unique experimental information about the equation of state (EoS) [1–4] as well as other equilibrium and nonequilibrium properties of nuclear matter far from its normal state [5–11]. Interpretation of the experimental results requires comparisons of data to predictions from transport models that take into account reaction dynamics. Transport models track the time evolution of a nuclear reaction and separately treat the nuclear EoS through the mean field part and the nucleon-nucleon (NN) collision cross sections through collisions. The influences of the mean field, both isospin-dependent and isospin-independent parts, and the NN collision cross sections have been studied using both the Boltzmann-Uehling-Uhlenbeck (BUU) and quantum molecular dynamics (QMD) approaches [12–14]. These studies also point out the importance of cluster formation in the description of reaction dynamics [2,12,13,15].

In the QMD model, fragments are formed due to A-body correlations caused by the overlapping wave packets. They are identified by the cluster recognition method, and play important roles in the final observables. At any time during the reaction process, fragments can be recognized by a minimum spanning tree (MST) algorithm [7,16]. In this algorithm, nucleons with relative distance of coordinate and momentum of $|r_i - r_j| \leqslant R_0$ and $|p_i - p_j| \leqslant P_0$ belong to a fragment. Here, r_i and p_i are the centroids of the wave packet for ith nucleon in their spatial and momentum space. R_0 and P_0 are phenomenological parameters determined by fitting the global experimental data, such as the IMF multiplicities [7,16]. They should roughly be in the range of nucleon-nucleon interaction. Typical values of R_0 and P_0 used in the QMD approaches are about 3.5 fm and 250 MeV/c [7,16]. This approach has been quite successful in explaining certain fragmentation observables, such as charge distributions of the emitted particles, IMF multiplicities [7,16–18], yield ratios of free neutrons to protons (n/p), and the double n/p ratios in heavy ion collisions [19]. On the other hand, the MST method fails to describe other details in the production of nucleons and light charged particles [7,16,20]. For example, while the yields of $Z = 1$ particles are overestimated, the yields of $Z = 2$ particles are underestimated partly due to the strong binding of α particles. Enhancements of the productions of neutron-rich isotopes observed in isoscaling [21], dynamically emitted heavy fragments [22] in neutron-rich HICs, and neutron-rich light charged particles (LCP) at midrapidity [23] have not been very described well by simulations using transport models. Furthermore, most transport models predict more transparency than that observed experimentally in central collisions at intermediate energy [12,24] due to insufficient production of fragments in the midrapidity region. Previous studies show that these problems cannot be resolved by changing only the mean field or nucleon-nucleon cross section in transport models.

There have been many attempts to improve the MST algorithm. More sophisticated algorithms such as the early cluster recognition algorithm (ECRA) [25], the simulated annealing clusterization algorithm (SACA) [26,27], and the minimum spanning tree procedure with binding energy of fragments (MSTB) [28] have been developed to provide better description of the IMF multiplicities or the average $Z_{\max}$ of the fragments. However, these algorithms do not address the lack of isospin dependence in cluster recognition, which is the main focus of this Rapid Communication.

In the regular MST method, neutrons and protons are treated equally in the cluster recognition process; a constant maximum distance for the nucleons to be defined as belonging to a cluster is $R_0^{nn} = R_0^{np} = R_0^{pp} = R_0 \sim 3.5$ fm. In order to investigate the effects of introducing the isospin dependence in the cluster recognition, the iso-MST, we choose different values of R_0^{nn}, R_0^{np}, and R_0^{pp}. We found that $R_0^{nn} = R_0^{np} = 6$ fm and $R_0^{pp} = 3$ fm give the largest effect on the heavy ion collision observables in this study. These values are consistent with the R_0 values ranging from 3 to 6 fm used in the QMD simulations in order to reproduce the cluster distribution reasonably. The larger distances of R_0^{nn} and R_0^{np} take into consideration of the properties of neutron-rich nuclei, such as neutron skin or neutron halo effect. Because of the long-range repulsive Coulomb force between protons in the cluster, a smaller R_0^{pp} value is adopted. $P_o = 250$ MeV/c is the same in both the MST and the iso-MST methods because nucleons with large relative

momentum are no longer close together in coordinate space after some time. In this Rapid Communication, we compare the results calculated with the MST and the iso-MST methods to investigate effects of introducing isospin dependence in the identification of cluster formation on isospin-sensitive observables. We also investigate how these cluster recognition methods affect the observable on system equilibrium. All of our studies are based on the improved quantum molecular dynamics model, ImQMD05 code [16–19].

Within the ImQMD05 approach, nucleons are represented by Gaussian wave packets, and the mean field acting on these wave packets is derived from an energy functional with the potential energy U that includes the full Skyrme potential energy without the spin-orbit term:

$$U = U_\rho + U_{md} + U_{\rm coul}, \tag{1}$$

where $U_{\rm coul}$ is the Coulomb energy. The nuclear contributions are represented in a local form with

$$U_{\rho,md} = \int u_{\rho,md} d^3r \tag{2}$$

and

$$\begin{aligned} u_\rho = {} & \frac{\alpha}{2}\frac{\rho^2}{\rho_0} + \frac{\beta}{\eta+1}\frac{\rho^{\eta+1}}{\rho_0^\eta} + \frac{g_{\rm sur}}{2\rho_0}(\nabla\rho)^2 \\ & + \frac{g_{\rm sur,iso}}{\rho_0}[\nabla(\rho_n-\rho_p)]^2 \\ & + \frac{C_s}{2}\left(\frac{\rho}{\rho_0}\right)^{\gamma_i}\delta^2\rho + g_{\rho\tau}\frac{\rho^{8/3}}{\rho_0^{5/3}}. \end{aligned} \tag{3}$$

Here, δ is the isospin asymmetry. $\delta = (\rho_n - \rho_p)/(\rho_n + \rho_p)$, and ρ_n and ρ_p are the neutron and proton densities, respectively. A symmetry potential energy density of the form $\frac{C_s}{2}(\frac{\rho}{\rho_0})^{\gamma_i}\delta^2\rho$ is used in the following calculations. In the present work, we adopt the value of $\gamma_i = 0.5$ (asy-soft EoS), which provides better agreement with data [19,29]. The energy density associated with the mean-field momentum dependence is represented by

$$\begin{aligned} u_{md} = {} & \frac{1}{2\rho_0}\Sigma_{N1}\frac{1}{16\pi^6}\int d^3p_1 d^3p_2 f_{N1}(\vec{p}_1) f_{N2}(\vec{p}_2) \\ & \times 1.57[\ln(1+5\times10^{-4}(\Delta p)^2)]^2, \end{aligned} \tag{4}$$

where f_N are nucleon Winger functions, $\Delta p = |\vec{p}_1 - \vec{p}_2|$, the energy is in MeV, and momentum is in MeV/c. The resulting interaction between wave packets is described in Ref. [7]. In this work, the $\alpha = -356$ MeV, $\beta = 303$ MeV, $\eta = 7/6$, $g_{\rm sur} = 19.47\,{\rm MeV\,fm^2}$, $g_{\rm sur,iso} = -11.35\,{\rm MeV\,fm^2}$, $C_s = 35.19$ MeV, and $g_{\rho\tau} = 0$ MeV. These calculations use isospin-dependent in-medium nucleon-nucleon scattering cross sections in the collision term, and the Pauli blocking effects are described in Refs. [16–18].

Figure 1(a) shows results of charge distributions from the central collisions of ^{124}Sn $+^{124}$ Sn at $b = 2$ fm at 50 MeV per nucleon beam energy calculated in the MST (open circles) and the iso-MST (solid circles), respectively. In the current paper, we adopt the convention that open circles are results obtained with the MST method and solid circles represent results using the iso-MST method, except in Fig. 4. Figure 1(b) plots the

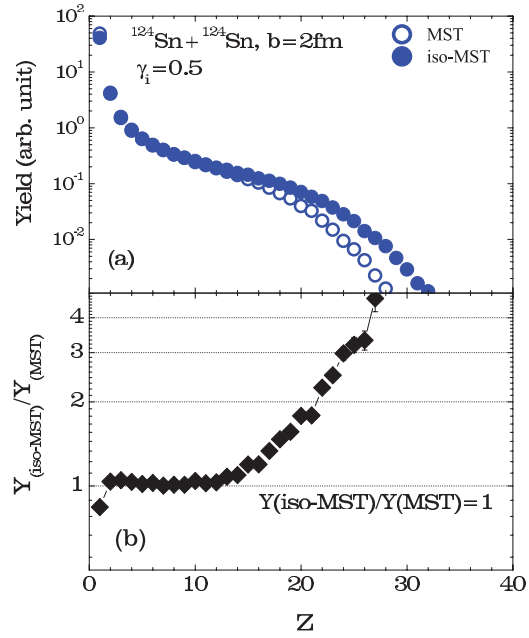

FIG. 1. (Color online) (a) Charge distribution of ^{124}Sn $+^{124}$ Sn at beam energy of $E/A = 50$ MeV for $b = 2$ fm for $\gamma_i = 0.5$. The solid circles are results from the iso-MST algorithm and the the open circles for the same reaction system. (b) Y(iso-MST)/Y(MST) ratio obtained from the same reaction system.

yield ratios from the iso-MST and the MST algorithms, that is, Y(iso-MST)/Y(MST). Since larger values of R_0^{nn} and R_0^{np} are adopted, more nucleons, especially neutrons, are included in clusters. As a consequence, the multiplicities of $Z = 1$ particles are reduced by about 16%, and the production of heavier fragments with $Z > 12$ are strongly enhanced. This may explain the strong enhancement of dynamically emitted heavy fragments observed in neutron-rich heavy ion collisions [22]. Even for intermediate mass fragments with $Z = 2$–12, the multiplicities are enhanced by ∼3%. In all cases, the enhancement is larger in neutron-rich heavy ion collisions.

In order to understand the enhancement of neutron-rich particles, we analyze the rapidity distributions of the particles emitted in central collisions of ^{124}Sn $+^{124}$ Sn reactions at $b = 2$ fm and incident energy of $E/A = 50$ MeV using both the MST (open circles) and the iso-MST (solid circles) algorithms. In Fig. 2, we present the rapidity distributions of n, p, and their ratios in panels (a), (b), and (c), respectively. The calculations with the iso-MST method (solid circles) reduce the yields of both neutrons and protons over all rapidity regions relative to the results obtained with MST case, especially at midrapidity. However, the yield ratios, $Y(n)/Y(p)$ [Fig. 2 (c)] are enhanced at midrapidity and become smaller at forward and backward rapidity regions in the iso-MST case than in the MST case.

In Figs. 2(d), 2(e), and 2(f), we plot the rapidity distributions of t, ^{3}He, and their ratios, $Y(t)/Y(^3{\rm He})$, respectively. The t and ^{3}He yields are much lower than those of n and p. Note that the scales of the y axis for Figs. 2(d) and 2(e) are a factor of 10 smaller than those in Figs. 2(a) and 2(b). Unlike the neutron yields, the triton yields [Fig. 2(d)] obtained with the iso-MST method are enhanced at midrapidity and remain

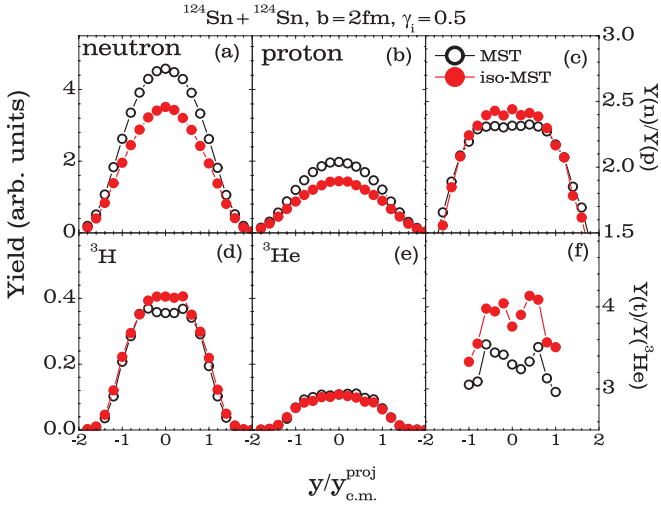

FIG. 2. (Color online) The rapidity distributions of (a) the neutron yields, (b) the proton yields, (c) the yield ratios, $Y(n)/Y(p)$, (d) the t yields, (e) the ^{3}He yields, and (f) the yield ratios, $Y(t)/Y(^3\mathrm{He})$.

nearly the same in the projectile or target regions relative to the results obtained with the MST method. On the other hand, there is very little difference in the yields of proton-rich ^{3}He [Fig. 2(e)] obtained with the iso-MST and the MST methods over the whole rapidity regions. As a consequence, the yields ratios, $Y(t)/Y(^3\mathrm{He})$, are much enhanced as shown in Fig. 2(f). The values of $Y(t)/Y(^3\mathrm{He})$ obtained with the iso-MST method increase to about 4.0 at midrapidity, much higher than the $Y(n)/Y(p)$ ratios. Two factors contribute to the larger $Y(t)/Y(^3\mathrm{He})$ ratios at midrapidity. First, the emitted nucleons at midrapidity have lower kinetic energy, because most of them pass through the expansion phase and dissipate their kinetic energy. At the end of the simulations, the emitted nucleons with lower kinetic energy are closer to the other clusters. Thus, the iso-MST algorithm with larger R_0^{nn} and R_0^{np} values will reduce the yields of nucleons at midrapidity as more nucleons close to the clusters are absorbed into fragments. Furthermore, production of neutron-rich fragments is enhanced at midrapidity due to larger $R_0^{nn/np}$ values adopted in the iso-MST case. The calculated results in Fig. 2 clearly demonstrate that cluster recognition method changes the yields of nucleons, light charged particles, and neutron-rich particles emitted at midrapidity in heavy ion collisions.

We also analyze the influence of the isospin-dependent cluster recognition method on isospin-dependent observables, such as $R(n/p) = Y(n)/Y(p)$, $DR(n/p)$, $R(t/^3\mathrm{He})$, and $DR(t/^3\mathrm{He})$ at lower and higher kinetic energy regions. In Table I, we list the yield ratios of n/p and $t/^3He$ with $E_k \leqslant 40$ MeV and $E_k \geqslant 40$ MeV for the neutron-rich reaction system ^{124}Sn $+^{124}$ Sn. It is clear that the iso-MST case increases the values of $R(n/p)$ at lower kinetic energy relative to the MST case. To reduce systematic uncertainties in experiments, we also construct the double ratios $DR(n/p)$ obtained from two reaction systems ^{124}Sn $+^{124}$ Sn, ^{112}Sn $+^{112}$ Sn at $b = 2$ fm using both the iso-MST and the MST algorithms. Here

$$DR(n/p) = \frac{[Y(n)/Y(p)]_{^{124}\mathrm{Sn}+^{124}\mathrm{Sn}}}{[Y(n)/Y(p)]_{^{112}\mathrm{Sn}+^{112}\mathrm{Sn}}}. \quad (5)$$

TABLE I. The calculated results of $R(n/p)$ and $R(t/^3\mathrm{He})$ obtained for ^{124}Sn $+^{124}$ Sn at $b = 2$ fm. The results of $DR(n/p)$, $DR(t/^3\mathrm{He})$, and α are obtained with an angular gate of $70^\circ \leqslant \theta_{\mathrm{c.m.}} \leqslant 110^\circ$ from two reaction systems (^{124}Sn $+^{124}$Sn and ^{112}Sn $+^{112}$Sn) at $b = 2$ fm.

Observable[a]	MST	iso-MST
$R(n/p)_{E_k<40\ \mathrm{MeV}}(^{124}\mathrm{Sn})$	2.131 ± 0.005	2.302 ± 0.006
$R(n/p)_{E_k>40\ \mathrm{MeV}}(^{124}\mathrm{Sn})$	1.044 ± 0.011	1.041 ± 0.011
$DR(n/p)_{E_k<40\ \mathrm{MeV}}$	1.514 ± 0.005	1.641 ± 0.006
$DR(n/p)_{E_k>40\ \mathrm{MeV}}$	1.803 ± 0.029	1.852 ± 0.030
$R(t/^3\mathrm{He})_{^{124}\mathrm{Sn}}$	3.031 ± 0.026	3.497 ± 0.028
$DR(t/^3\mathrm{He})_{E_k/A<40\ \mathrm{MeV}}$	1.57 ± 0.02	1.64 ± 0.02
Isoscaling parameter α	0.19	0.22

[a]All the results are obtained with $\gamma_i = 0.5$ case.

For nucleons with low kinetic energy (<40 MeV), $DR(n/p)$ obtained in the iso-MST case is larger by about 8.3%. For nucleons with high kinetic energy (>40 MeV), the difference between the $DR(n/p)$ values obtained from both the MST and the iso-MST cases is much less. As most of the emitted triton and ^{3}He have kinetic energies less than 40 MeV per nucleon, we list the $R(t/^3\mathrm{He})$ and $DR(t/^3\mathrm{He})$ values with $E_k/A < 40$ MeV in the fifth and sixth rows of Table I. The iso-MST algorithm enhances the $R(t/^3\mathrm{He})$ and $DR(t/^3\mathrm{He})$ values more than $R(n/p)$ and $DR(n/p)$.

With larger R_0^{nn} and R_0^{np} values adopted in the iso-MST method, more neutron-rich isotopes are produced. This effect is further enhanced in the neutron-rich reaction system. Figure 3 shows the isotope distributions of primary fragments with $Z = 3$ to 8 predicted by the ImQMD05 calculations over the angle region, $70^\circ \leqslant \theta_{\mathrm{c.m.}} \leqslant 110^\circ$ for ^{124}Sn $+^{124}$ Sn system. The solid circles are results obtained with the iso-MST method, and open circles are results obtained with the MST method.

The isoscaling relationship, which is constructed using isotope yields $Y_i(N, Z)$ with neutron number N and proton number Z from two different reaction systems denoted by the

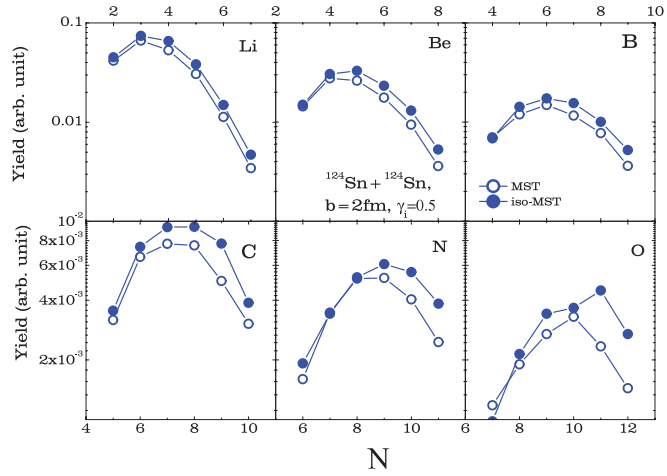

FIG. 3. (Color online) Calculated primary isotope yields of Li, Be, B, C, N, and O for ^{124}Sn $+^{124}$ Sn with an angular gate of $70^\circ \leqslant \theta_{\mathrm{c.m.}} \leqslant 110^\circ$ for $\gamma_i = 0.5$ at $b = 2$ fm.

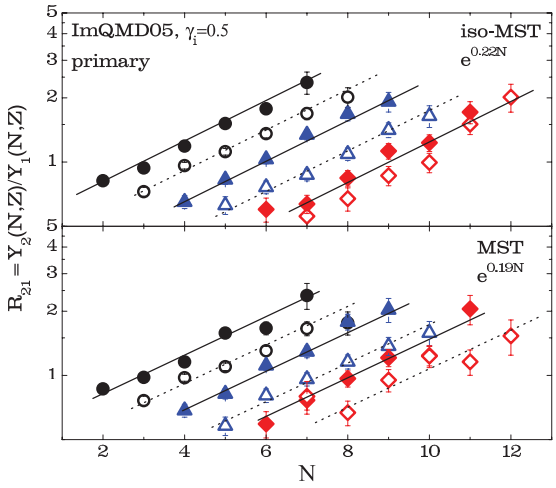

FIG. 4. (Color online) R_{21} values obtained from the ratios of the primary isotopic distributions for ^{124}Sn $+^{124}$ Sn collisions divided by those for ^{112}Sn $+^{112}$ Sn collisions, for $\gamma_i = 0.5$ at $b = 2$ fm. The upper panel shows the results obtained with the iso-MST case for $Z = 3$ to 8, and the lower panel shows the results obtained with the MST case for $Z = 3$ to 8. The best-fit isoscaling parameters are listed in the panels.

index i, obeys a simple relationship:

$$R_{21}(N, Z) = Y_2(N, Z)/Y_1(N, Z) = C\exp(\alpha N + \beta Z). \quad (6)$$

Here, C is an overall normalized factor and α and β are isoscaling parameters. The isoscaling parameter α can be used to estimate the enhancement of neutron-rich isotopes and has been used as a probe to study the density dependence of symmetry energy [21,30–32]. We analyze the isoscaling relationship with both cluster recognition methods for fragments with $Z = 3$–8. In Fig. 4, as an example, we plot the $R_{21} = Y_2/Y_1$ values as a function of N of the emitted fragments obtained with the iso-MST and the MST cases. Here, "2" represents the neutron-rich reaction system ^{124}Sn $+^{124}$ Sn, and "1" represents ^{112}Sn $+^{112}$ Sn. The upper panel shows the results obtained with the iso-MST case, and the lower panel shows results obtained with the MST case. As in a previous study [15], we find that the isoscaling relationship exists in a nonequilibrium transport model. The best fit isoscaling parameters α are listed on the figure and in Table I. The isoscaling parameter α obtained with the MST is 0.19, and the α value obtained with the iso-MST case increases to 0.22, which is still less than the experimental value of $\alpha = 0.36 \pm 0.04$ [31]. Sequential decays may modify the α values. However, results from current sequential decay calculations are model dependent [33,34]. Since the differences in α values are small, it will be difficult to determine the exact effects until more realistic sequential model calculations become available.

Finally, we examine the effects of isospin cluster recognition on the system equilibrium measured by the production of light particles. To characterize the degree of equilibrium reached in the collision system, the observable of $vartl = \sigma^2_{\rm trans}/\sigma^2_{\rm long}$ is often used in experimental and theoretical studies [17,18,35]. Here, the $\sigma^2_{\rm tran}$ and $\sigma^2_{\rm long}$ are the variance

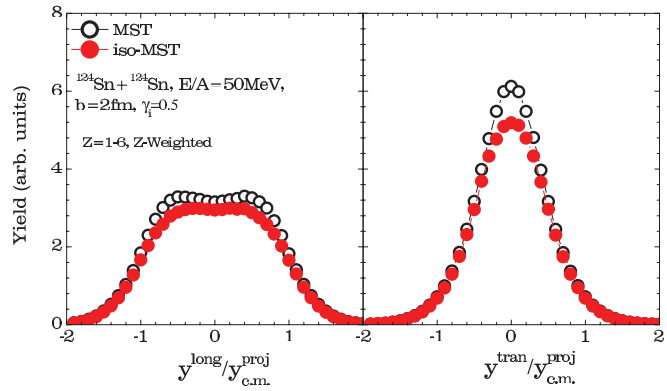

FIG. 5. (Color online) The calculated results of longitudinal (left panel) and transverse (right panel) rapidity distribution for the Z-weighted yield ($Z = 1$–6) for ^{124}Sn $+^{124}$ Sn at $b = 2$ fm.

of transverse and longitude rapidity distributions of fragment yields. When the reaction system reaches equilibrium, the value of *vartl* is close to 1. In Fig. 5, we plot the calculated results of longitudinal (left panel) and transverse (right panel) rapidity distributions for the Z-weighted yield ($Z = 1$–6) for ^{124}Sn $+^{124}$ Sn at $b = 2$ fm. The much wider longitudinal rapidity distributions suggest that the systems are far from equilibrium. More interestingly, the peaks in the longitudinal rapidity distribution (left panel) for $Z = 1$–6 particles obtained in the MST case diminishes in the iso-MST case. It suggests that a higher degree of equilibrium is predicted in the iso-MST case. With $\gamma_i = 0.5$, the value of $vartl = \sigma^2_{\rm trans}/\sigma^2_{\rm long}$ obtained with the iso-MST case is 0.62, which is slightly larger than 0.58 for the MST case. Thus in addition to the isospin-sensitive observables, the equilibrium or stopping power of the system also depends on the detailed description of cluster formation implemented in the transport models as well as on the mean field and the in-medium NN cross section.

In summary, we introduce a phenomenological isospin dependence in the description of cluster formation in transport models by adopting different R_0 values for pp, nn, and np, $R_0^{pp} = 3$ fm and $R_0^{nn} = R_0^{np} = 6$ fm. Our results using the isospin-dependent minimum spanning tree method show suppression of $Z = 1$ particles and enhancement of fragments, especially for heavier fragments with $Z \geqslant 12$. Furthermore, we find enhanced production of neutron-rich isotopes at midrapidity. Consequently, isospin-sensitive observables, such as the double ratios, $DR(t/^3\mathrm{He})$, and isoscaling parameter α increase to larger values. The widths of the longitudinal and transverse rapidity distributions of $Z = 1$–6 particles also change. In all the observables that we examine, the effects introduced by the iso-MST algorithm are relatively small but in the direction of better agreement with data. However, we have not included sequential decays, which may modify the magnitude of the effects. Nonetheless, the isospin dependence of the cluster recognition can be easily implemented and should be included in nuclear transport models.

This work has been supported by the Chinese National Science Foundation under Grants No. 11075215, No. 10979023, No. 10875031, No. 11005022, No. 11005155,

and No. 10235030, and the national basic research program of China, Grant No. 2007CB209900. We acknowledge the support of the National Science Foundation, Grant No. PHY-0606007.

[1] B. A. Brown, Phys. Rev. C **43**, R1513 (1991).
[2] M. B. Tsang, Y. Zhang, P. Danielewicz, M. Famiano, Z. Li, W. G. Lynch, and A. W. Steiner, Phys. Rev. Lett. **102**, 122701 (2009).
[3] P. Danielewicz, R. Lacey, and W. G. Lynch, Science **298**, 1592 (2006).
[4] B. Li, L. W. Chen, and C. M. Ko, Phys. Rep. **464**, 113 (2008).
[5] J. P. Bondorf, A. S. Botvina, A. S. Iljinov, I. N. Mishustin, and K. Sneppen, Phys. Rep. **257**, 133 (1995).
[6] D. H. E. Gross, Rep. Prog. Phys. **53**, 605 (1990).
[7] J. Aichelin, Phys. Rep. **202**, 233 (1991).
[8] M. Colonna, G. Fabbri, M. Di Toro, F. Matera, and H. H. Wolter, Nucl. Phys. A **742**, 337 (2004).
[9] P. Chomaz, M. Colonna, and J. Randrup, Phys. Rep. **389**, 263 (2004).
[10] A. Le Fevre and J. Aichelin, Phys. Rev. Lett. **100**, 042701 (2008).
[11] C. B. Das, S. Das Gupta, W. G. Lynch *et al.*, Phys. Rep. **406**, 1 (2005).
[12] Y. Zhang, D. D. S. Coupland, P. Danielewicz *et al.*, Phys. Rev. C **85**, 024602 (2012).
[13] D. D. S. Coupland, W. G. Lynch, M. B. Tsang, P. Danielewicz, and Y. Zhang, Phys. Rev. C **84**, 054603 (2011).
[14] B.-A. Li and L.-W. Chen, Phys. Rev. C **72**, 064611 (2005).
[15] A. Ono, P. Danielewicz, W. A. Friedman, W. G. Lynch, and M. B. Tsang, Phys. Rev. C **68**, 051601(R) (2003).
[16] Y. Zhang and Z. Li, Phys. Rev. C **71**, 024604 (2005).
[17] Y. Zhang and Z. Li, Phys. Rev. C **74**, 014602 (2006).
[18] Y. Zhang, Z. Li, and P. Danielewicz, Phys. Rev. C **75**, 034615 (2007).
[19] Y. Zhang, P. Danielewicz, M. Famiano, Z. Li, W. G. Lynch, and M. B. Tsang, Phys. Lett. B **664**, 145 (2008).
[20] R. Nebauer *et al.*, Nucl. Phys. A **658**, 67 (1999).
[21] T. X. Liu, M. J. v an Goethem, X. D. Liu, W. G. Lynch *et al.*, Phys. Rev. C **69**, 014603 (2004).
[22] P. Russoto, E. De Filippo, A. Pagano *et al.*, Phys. Rev. C **81**, 064605 (2010).
[23] Z. Kohley, L. W. May, S. Wuenschel *et al.*, Phys. Rev. C **83**, 044601 (2011).
[24] S. Hudan, A. Chbihi, J. D. Frankland *et al.*, Phys. Rev. C **67**, 064613 (2003).
[25] C. O. Dorso and J. Randrup, Phys. Lett. B **301**, 328 (1993).
[26] R. K. Puri and J. Aichelin, J. Comput. Phys. **162**, 245 (2000).
[27] P. B. Gossiaux, R. K. Puri, C. Hartnack, and J. Aichelin, Nucl. Phys. A **619**, 379 (1997).
[28] S. Goyal and R. K. Puri, Phys. Rev. C **83**, 047601 (2011).
[29] Z. Y. Sun *et al.*, Phys. Rev. C **82**, 051603(R) (2010).
[30] H. S. Xu, M. B. Tsang, T. X. Liu, X. D. Liu, W. G. Lynch *et al.*, Phys. Rev. Lett. **85**, 716 (2000).
[31] M. B. Tsang, C. K. Gelbke, X. D. Liu, W. G. Lynch *et al.*, Phys. Rev. C **64**, 054615 (2001).
[32] S. R. Souza, M. B. Tsang, B. B. Carlson *et al.*, Phys. Rev. C **80**, 041602(R) (2009).
[33] M. B. Tsang, R. Bougault, R. Charity *et al.*, Eur. Phys. J. A **30**, 129 (2006); **32**, 243 (2007).
[34] M. Colonna, V. Baran, M. Di Toro, and H. H. Wolter, Phys. Rev. C **78**, 064618 (2008).
[35] W. Reisdorf *et al.* (FOPI Collaboration), Phys. Rev. Lett. **92**, 232301 (2004).